

5-24-2023

## Betaglycan promoter activity is differentially regulated during myogenesis in zebrafish embryo somites

Lizbeth Ramírez-Vidal

Tonatiuh Molina-Villa

Valentín Mendoza

Carlos Alberto Peralta-Álvarez

Augusto Cesar Poot-Hernández

*See next page for additional authors*

Follow this and additional works at: <https://digitalcommons.unomaha.edu/biomechanicsarticles>



Part of the [Biomechanics Commons](#)


Please take our feedback survey at: [https://unomaha.az1.qualtrics.com/jfe/form/SV\\_8cchtFmpDyGfBLE](https://unomaha.az1.qualtrics.com/jfe/form/SV_8cchtFmpDyGfBLE)

---

**Authors**

Lizbeth Ramírez-Vidal, Tonatiuh Molina-Villa, Valentín Mendoza, Carlos Alberto Peralta-Álvarez, Augusto Cesar Poot-Hernández, Dobromir Dotov, and Fernando López-Casillas

# Betaglycan promoter activity is differentially regulated during myogenesis in zebrafish embryo somites

Lizbeth Ramírez-Vidal<sup>1</sup> | Tonatiuh Molina-Villa<sup>1</sup> | Valentín Mendoza<sup>1</sup> | Carlos Alberto Peralta-Álvarez<sup>2</sup> | Augusto Cesar Poot-Hernández<sup>2</sup> | Dobromir Dotov<sup>3</sup> | Fernando López-Casillas<sup>1</sup> 

<sup>1</sup>Departamento de Biología Celular y del Desarrollo, Instituto de Fisiología Celular, UNAM, Mexico City, Mexico

<sup>2</sup>Unidad de Bioinformática y Manejo de la Información, Instituto de Fisiología Celular, UNAM, Mexico City, Mexico

<sup>3</sup>Psychology, Neuroscience & Behaviour, McMaster University, Hamilton, Canada

## Correspondence

Fernando López-Casillas, Department of Cellular and Developmental Biology, Institute of Cellular Physiology, UNAM, Universidad Nacional Autónoma de México, Circuito Exterior s/n, Ciudad Universitaria, Coyoacán, México City, México.

Email: [fcasilla@ifc.unam.mx](mailto:fcasilla@ifc.unam.mx)

## Funding information

Consejo Nacional de Ciencia y Tecnología, Grant/Award Number: 254046; Dirección General de Asuntos del Personal Académico, Universidad Nacional Autónoma de México, Grant/Award Numbers: IN204620, IN204916

## Abstract

**Background:** Betaglycan, also known as the TGF $\beta$  type III receptor (Tgfr3), is a co-receptor that modulates TGF $\beta$  family signaling. Tgfr3 is upregulated during C2C12 myoblast differentiation and expressed in mouse embryos myocytes.

**Results:** To investigate *tgfr3* transcriptional regulation during zebrafish embryonic myogenesis, we cloned a 3.2 kb promoter fragment that drives reporter transcription during C2C12 myoblasts differentiation and in the *Tg(tgfr3:mCherry)* transgenic zebrafish. We detect *tgfr3* protein and mCherry expression in the adaxial cells concomitantly with the onset of their radial migration to become slow-twitch muscle fibers in the *Tg(tgfr3:mCherry)*. Remarkably, this expression displays a measurable antero-posterior somitic gradient expression.

**Conclusions:** *tgfr3* is transcriptionally regulated during somitic muscle development in zebrafish with an antero-posterior gradient expression that preferentially marks the adaxial cells and their descendants.

## KEYWORDS

adaxial cells, antero-posterior gradient zebrafish myogenesis, betaglycan, slow twitch somitic muscle, Tgfr3 gene promoter

## 1 | INTRODUCTION

Betaglycan, also known as the TGF $\beta$  type III receptor, TGFBR3, is a plasma membrane proteoglycan that modulates the access of some members of the TGF $\beta$  family to their signaling cognate type I and II receptors. In vitro work has revealed an array of TGFBR3 functions such as enhancement of the TGF $\beta$ 2 binding and potency,<sup>1</sup> and its role in the inhibin A antagonism of activin signaling.<sup>2,3</sup> Additionally, TGFBR3 ectodomain shedding results in

the release of the TGF $\beta$ -neutralizing “soluble betaglycan,”<sup>4-10</sup> and the fact that TGFBR3 heparan sulfate chains bind bFGF and other growth factors adds to its functional diversity.<sup>11-13</sup> However, none of these biochemical properties account for the embryonic lethality of *Tgfr3* knockout mice, who die during midgestation (E14.5-16.5), showing ventricular septal defects, liver apoptosis and defective hematopoiesis.<sup>14</sup> Defective and hypoplastic coronary arteries have also been reported, apparently due to decreased proliferation and invasion of

This is an open access article under the terms of the [Creative Commons Attribution-NonCommercial](https://creativecommons.org/licenses/by-nc/4.0/) License, which permits use, distribution and reproduction in any medium, provided the original work is properly cited and is not used for commercial purposes.

© 2023 The Authors. *Developmental Dynamics* published by Wiley Periodicals LLC on behalf of American Association for Anatomy.

epicardium and endocardium, a process that has been linked to TGFBR3 participation in a non-canonical NF- $\kappa$ B signaling pathway.<sup>15,16</sup> Although it was proposed that the defects seen in the *Tgfr3* null mice were caused by improper TGF $\beta$ 2 signaling, it is clear that the *Tgfb2* null mice do not faithfully phenocopy the *Tgfr3* null phenotype.<sup>17</sup> Recent work from our laboratory indicates that *tgfr3* downregulation in zebrafish embryos using morpholino oligonucleotides causes non-cell autonomous angiogenesis defects and improper arrangement of actin fibers in the posterior somites which exhibit a rounder appearance.<sup>18</sup> Nonetheless, the *tgfr3* null zebrafish does not phenocopy the drastic defects observed in the morphant, adding to the complexity of Tgfr3 biology and suggesting some type of genetic compensation in the null fish or an off target morpholino effect.<sup>19</sup> To gain deeper insights into these findings we report the identification of the zebrafish *tgfr3* promoter and its activity during the development of somitic skeletal muscle.

## 2 | RESULTS

### 2.1 | Zebrafish *tgfr3* gene structure and identification of exon 1

Blast analysis of the reported zebrafish *tgfr3* cDNA (GenBank accession number KF17096) over the Ensembl GRCz10 database, identified and aligned with 15 exons that expand from about nucleotide 24 320 000 to 24 500 000 on the plus strand of chromosome 6. From this alignment exons 2 to 16 can be unequivocally identified over their corresponding chromosome 6 sequences (Figure 1A), clearly showing a similar pattern to *Tgfr3* genes in mammals and predicts the existence of a putative first exon which is absent from the cDNA clone KF17096.

To identify the missing first exon, we searched GRCz10 for expressed sequence tags (EST) and found the EST clone EB978660, which contains the complete exon

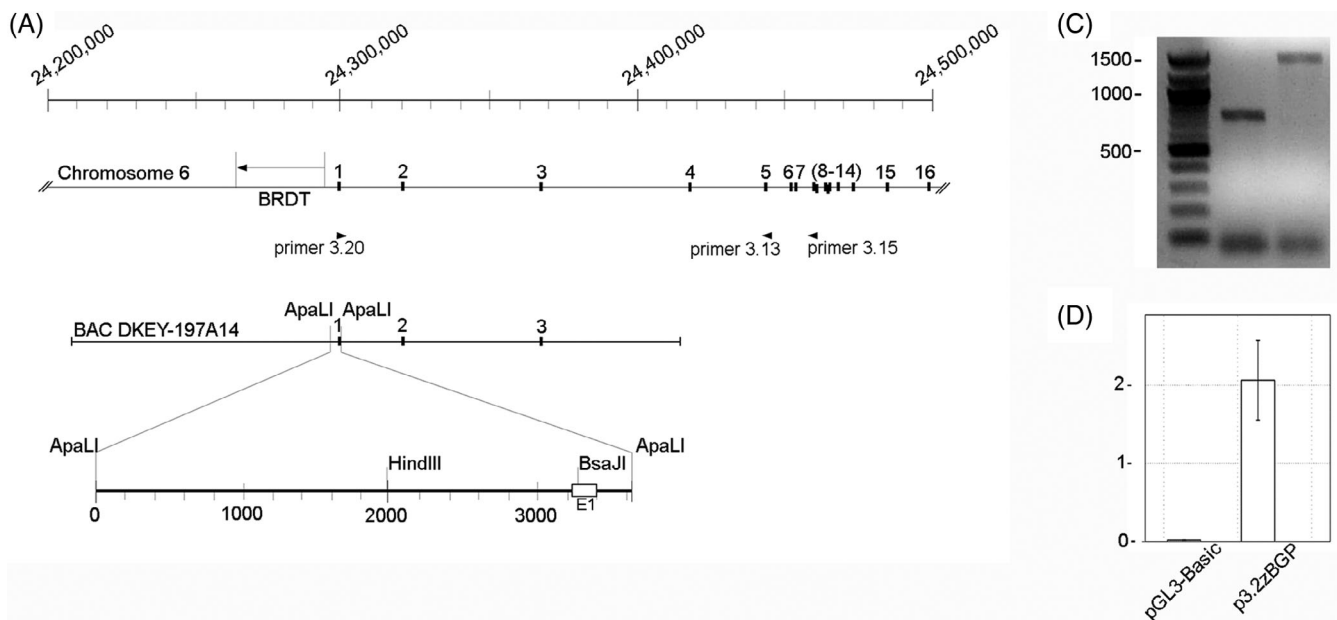


**FIGURE 1** Zebrafish *Tgfr3* gene map, exon 1 assignment and promoter sequence and activity. (A) The 16 *Tgfr3* exons are shown as black numbered rectangles on the line representing of the 300 000 bp in *Danio rerio* chromosome 6 containing the *Tgfr3* gene. The location of the testis-specific bromodomain gene (BRDT), transcribed from the opposite strand, is indicated. The position of the bacterial artificial chromosome (BAC) DKEY-197A14 and its zoomed-in ApaLI-ApaLI fragment containing the BG promoter are shown. Positions of primers 3.20, 3.13, and 3.15, located in exons 1, 5, and 9, respectively, are indicated by arrowheads. (B) Zebrafish *Tgfr3* promoter nucleotide sequence. The nucleotide sequence of the ApaLI-ApaLI fragment containing the *Tgfr3* promoter and first exon is shown. Positive ascending numbers on the right are from upstream ApaLI to downstream ApaLI sites. Negative descending numbers on the left are upstream from the sequences assigned as exon 1 (bold italics); nucleotides belonging to following intron 1 are shown in lower case letters. Position of primer 3.20 is indicated by dotted underline. Relevant responsive elements identified by Mat Inspector are underlined and named. Position of relevant restriction sites are indicated with their names above the sequence. (C) The RT-PCR products obtained with primers 3.20 to 3.13 (lane 1) and primers 3.20 to 3.15 (lane 2) are separated, along with 100-bp molecular markers ladder (lane M), by electrophoresis in an agarose gel. (D) The graph shows the beta-galactosidase-normalized luciferase activity obtained upon transfection of ZF4 fibroblasts with the promoter-less pGL3-basic plasmid or its derivate, p3.2tgfr3:luc, which contains the ApaLI-BsaJI 3260 bp fragment.

2, 124 bp of exon 3, and novel 228 bp upstream to the cloned cDNA, 168 of them are at the 5'-end and could correspond to the putative exon 1 (shown in bold italics in Figure 1B). To demonstrate that these sequences are a bona fide part of the *tgfr3* mRNA, we performed a RT-PCR amplification using bases 26 to 49 of the EST clone

EB978660 as the upstream primer (primer 3.20, dotted underline in Figure 1B) and as downstream primers 3.13 or 3.15, which anneal to sequences in exons 5 and 9, respectively (arrowheads in Figure 1A). This approach yielded PCR products of 740 and 1472 bp (Figure 1C), which have the sizes expected if generated from a

(B)

	<i>Apa LI</i>							
-3229	GTGCACCACA	CCAACATGTT	TTGGCAAAC	TTGTCTTTAT	CAGGATAACC	TATAATTATT		60
-3169	ACGTTTAATG	TATTAAATAT	TTAAATTTAT	ATTTTATTTT	CACAAACATC	ATTTGAAAAA		120
-3109	GTAACACTT	GAAATAATTT	CTGTGAATAA	ACAGTGATTT	TTTAATTGTT	ATTAAATGCA		180
-3049	GTACAAATTC	CCAAACAGGA	<b>CATCCTGTCT</b>	<b>TTAAGTCATG</b>	TCTATGCAAC	AATGTTACAT		240
			<b>ARE</b>					
-2989	ATGCAAAAGA	CTTGTTTAGG	ATTTCCATTT	GTCAATGCAG	<b>TACAATGAGT</b>	<b>GCATTATAAC</b>		300
					<b>GRE/ARE</b>			
-2929	GGATCATGCA	<b>TTGGAA</b> TTCC	CTGATATTCC	ATAGTTGATT	TTCTTCCCAA	TTATATTCGA		360
		<b>NFkB</b>						
-2869	TGTACCATTC	ATTTAATAAA	AAAGAAAAAC	AAAATGACTG	<b>ACAAAGAGAA</b>	<b>AGAATGCAAA</b>		420
					<b>Prdm1</b>			
					<b>Sox6</b>			
-2809	CAAACAAATG	AAATCAAAGA	ATTAGGGCAG	GGGAATCATG	TTCGGGACTG	GATTTTGTGG		480
-2749	CATCTCTCTT	TCCGCTGTG	CAGATGCTTT	GAGCAGGCCT	GCTTCAGAGG	CATACATATG		540
-2689	CATGAGAAGT	<b>GAAAGATGAC</b>	<b>ATGAAGCCTC</b>	TGTGTACATC	TTCATTGACA	CTCAAAAGCA		600
		<b>Prdm1</b>						
-2629	GCATATCAAT	GTTTCCAAGA	CAGCAAGAAG	<b>CTCCAAAACA</b>	<b>AAGTTTTCCA</b>	<b>TCTTGGAAGG</b>		660
					<b>Sox6</b>			
-2569	GTGCTGTCTC	ATTAGTGGCA	AATCACGACT	CTGACATTTA	CACTGTAAGC	AGTGCTAAAG		720
-2509	CATTTCCATT	TCCTTTAGAA	CGGAGCAGAA	<b>CATTTCACTC</b>	<b>AAACAACATA</b>	AGTCTGTTTG		780
				<b>Prdm1</b>				
-2449	TTCACGAAAA	AACAAGCCAG	AAGAGGAGGC	AGAGAGATAA	AAAAGAAAGA	AAATGCAAAT		840
-2389	<b>GAAA</b> AGTAA	ATATATCCTG	CAAAAACA <b>AA</b>	<b>TACACACAAA</b>	CATGAAATTT	AGCTTAAATA		900
	<b>Prdm1</b>			<b>Foxh1</b>				
-2329	CAATCATACC	ATTTTGTGTT	TGCTTTTTC	TTTGGCTCTT	AAAAGCAAAT	TGAACACACA		960
-2269	TGCAATGACC	AAATGCAACA	GTAAACACAA	TAAATGTTT	TATATCACTT	CAGTCGACGA		1020
-2209	CTTCTTCAAG	<b>TGAATTGTTG</b>	<b>ATTG</b> TAAAGG	CTTATTAATT	AGTTAATGAT	GTAATCAACT		1080
		<b>Fast1</b>						
-2149	AAATGACTCC	AAAGTCAAGA	TTTTGGTTAA	AGAGGTGTGT	TTGTGTCTAA	GAAAGCCAA		1140
-2089	ACTAAAGTCA	GGTCAACATG	TTTTCCTTGA	ATCAAATCAG	TTGGCAATGA	CAGAGTGATC		1200
-2029	CTGCTATCAC	TGAAAAATGT	AACAGATAAG	ATTTACTACA	TCTATGAAAT	CAGAGTAGAA		1260
-1969	<b>AGTAGTCTGG</b>	<b>ATAAAGATAT</b>	<b>TACTTTAGAT</b>	<b>AACACTTAGA</b>	<b>ACCTCATCCT</b>	<b>AATAGAGTTA</b>		1320

FIGURE 1 (Continued)

continuous mRNA linking the upstream sequence from the EB978660 EST to the exons 5 or 9. Further support that this sequence at the 5'-end of the EST EB978660 is a bona fide part of the *tgfr3* exon 1 is provided by the fact that it maps 21 kb upstream of the putative exon 2, which

contains the ATG codon that opens *tgfr3* mRNA reading frame (see Figure 1A). This arrangement is similar in the mammalian orthologous betaglycan genes whose second exons are located 23 to 24 kb downstream of exon 1. In summary, the nucleotide sequence of the RT-PCR

-1909	GGAAATATAA	TTTGCTTATG	TAAAATGCAT	TTTGTATTGG	TTGTCCTTGC	TTTAAAGTG	1380
-1849	<u>TCT<b>TTGT</b>TGC</u>	ACATTTTATA	AAGTAATTAC	AACTAATTCT	GCATAACCCA	AGACTTAACC	1440
	<b>Sox6</b>						
-1789	ACTTCCTAAC	TCTAAACATA	TCAAATACAT	<u>AT<b>CAAA</b>ATGT</u>	CAAATAATA	GTACATTGCA	1500
			<b>RAR<math>\gamma</math></b>				
-1729	ATGAATCTG	ATTTGTATCA	AATGAGGTTT	<u>ACAT<b>CTAT</b>TTT</u>	AAAGGATCTA	AATGTTATAG	1560
			<b>MEF2</b>				
-1669	TTGTCTCTCT	GAAAAATGTA	ATTTTCTGAT	TTAGGGTAAG	<u>GATCAGAACA</u>	<u>TTT<b>GTCT</b>GGT</u>	1620
					<b>MYF6</b>	<b>Smad3</b>	
-1609	<u>AGTTGCTTGA</u>	GATTGTGGCA	TCATTGGCTT	CACTTCAAAT	GAATTTATGA	TTATGATGAG	1680
-1549	CACATTTCCA	GGCTTTCAAA	ATAACAAACA	TAGTAAAAATG	TATTACATTA	<u>ACCTTA<b>TGTT</b></u>	1740
						<b>GRE</b>	
-1489	<u>CATTAAAAATG</u>	CAAGACAATG	CTTCACAGAA	AAGAAATGCA	TTTGAATATG	TATGGATGAA	1800
-1429	TAATCATATT	TTAAGATATT	TTGGAATGTA	CATTATTTAA	<u>AATACAGCAA</u>	<u>TC<b>CACT</b>AAAT</u>	1860
					<b>Foxh1</b>		
-1369	<u>TTATTGTAGT</u>	GGTTTATGCA	GTTTTGGTCA	AACATCTTTA	TTGTCATTTT	TATGATGTTT	1920
-1309	AAAAATTGGC	TGGATGTGGT	<u>GTGT<b>GAAAA</b></u>	GGTTAAAGGA	ACAAGATTAT	TCACAAAAGC	1980
			<b>Prdm1</b>				
-1249	TTAAAAAATG	ACAAATTCCA	CTAAATAAAA	GGTCTGTTGA	GAGGAACTAA	AAAGAAGAAT	2040
-1189	GGCAGAAGTT	<u>GCCTAA<b>AAAT</b></u>	AAATGTGCCA	TGCTTGTAGC	ATCATGCTCA	<u>AAAAGACTTG</u>	2100
		<b>MEF2C</b>					
-1129	<u>AGGT<b>TCT</b>AAAT</u>	<u>TGGT<b>GACAAA</b></u>	GGTGTTTATT	CATTTAAAAA	GCAACAAAAA	TAAATGAGCT	2160
	<b>ARE</b>	<b>Sox6</b>					
-1069	TTCAAATGAA	CTTCTTTCAT	GTAGGCATTA	TACTGTATTA	TTTTCAGAAT	TGTTTGGGAA	2220
-1009	ATATATTAAT	TTAATTAATT	TTGGAATACG	GCTTTAACAT	ATAATGTTGA	AAAAGGGCAC	2280
-949	AGATTAAACT	TTCCGGATGC	ACTATTTGTC	AATTCCTACT	CATTTCATAG	CTATAATGGC	2340
-889	AAAACAAAACA	AACAAACAAA	CAAATAAAAA	AACAACAACA	AAATAAAGAT	GACGATTATT	2400
-829	ATTATGATAA	TGATTATTGT	TATTGTTTAT	ACTATTTAGG	TAAAACAACA	AACAAAAAGC	2460
-769	AAACAATGAT	TCAAATAAAA	ACTAAACAAA	TAAATAATGA	ATAATAATAA	TAAATATTAC	2520
-709	AACAAAACAA	AACCACAACA	ATAATGAATA	TTATTACATG	TAATAAAAAAT	AATACGAAAA	2580
-649	CAACAACAAA	ATGTAATTAT	TAATAATGCT	AGTAATACTA	AATATAACAA	CAAAACAACA	2640
-589	ACAAAATAAA	GATGCTACAA	TTAAACAACA	AAAACAACAA	CAAAAACAAC	AACAATAATA	2700

FIGURE 1 (Continued)



product, and the conserved distribution of exons and introns support our assignment as the exon 1 of the *tgfb3* gene, predicting that the upstream region is the promoter.

## 2.2 | Zebrafish *tgfb3* gene promoter cloning

To clone the promoter of the *tgfb3* gene, we used the BAC DKEY-197A14 (Bacterial Artificial Chromosome, GenBank: CU137682.11), which encompasses 205 390 bp of chromosome 6 including *tgfb3* exons 1 to 3 and upstream sequence. We sequenced a 3634 bp ApaLI fragment from this BAC and found that bases 3229 to 3397 align with the 5' end of the EB978660 EST clone (Figure 1A,B), the putative first exon of the zebrafish *tgfb3* gene. Upstream, these bases are flanked by 3229 bp of the putative promoter, and downstream, by the

beginning of the first intron of the gene. To test its transcriptional activity, the 3260 bp-long ApaLI-BsaJI fragment, containing 30 bp of the first exon plus 3229 bp corresponding to its upstream putative promoter, was subcloned in the luciferase-encoding pGL3-basic plasmid and the created reporter, p3.2*tgfb3*:luc, was assayed in ZF4 zebrafish embryonic fibroblasts.<sup>20</sup> Strong luciferase activity was observed with p3.2*tgfb3*:luc but not with empty pGL3-basic plasmid 72 hours post transfection (hpf), (Figure 1D), indicating that this sequence is transcriptionally active.

MatInspector analysis<sup>21</sup> (Genomatix software suite, v3.7) revealed that the ApaLI-BsaJI fragment sequence lacks a TATA binding element, but contains a SP1-GC-Box, which is located at a position (−63 to −58) suitable to set transcription initiation just 5' to the assigned exon 1 (Figure 1B). This finding is in agreement with the fact that *Tgfb3* genes of rat and mouse have TATA-less promoters containing GC box and SP1 binding sites.<sup>22,23</sup>

-529	ACAATAAATA CAATAATCAT AATAATAATA TCAATAATAA TAATAATAAT AATAATAACA	2760
-469	ATAATAATAA TAATAATAAT AATAATAATA AAAGTAATAA TTTTATTAAG GTAAAACCAG	2820
-409	<u>CAAATAACA ACAACAACAA CGGTGATAAA AATTAAATAA AATATGAATA ATAATAATAA</u>	2880
	<b>Fast1</b>	
-349	TTATTATATA AAAACATAAT CAATAATAAT GTAATAATAA TAATAATAAT AATAATTTAT	2940
-289	TCTTCTTATT CTAATAATAA TAATAATAAT AATAATAATA ATAATAATAA TAATAATAAT	3000
-229	AATTATTATT ATTATTATAT TTTGTTATTA TTATATATGC TGTAGACAGT TGTACAAGTA	3060
-169	AATTTAGTAT CATGCTGGCG GAAGTAGAAG GGGTTTCAAG CCCACTTCAT CCTCAGTTTT	3120
-109	TTTTTTTTTC ATGATAGATG TGAATCTCAA CCTCCTCCTA <u>CTGGCCCCCTC CCACTAAAAC</u>	3180
	<b>Sp1</b>	
	<b>+1 &gt; exon1</b>	
-49	GCACAGAGAG <u>ACA</u> <b>GAAAGCG</b> GGAGAGGTAT TTAAAACTTT TTGAGA <b>ACTG TCACAGGCTT</b>	3240
	<b>Prdm1</b> <b>Sox6</b>	
	<i>Bsa JI</i>	
	<u>TGTCATCCCG AAAACCGTGG CGTTTGTTCG GGTATTAATT AGTATACAAA CAGAAGTGTA</u>	3300
	<b>TACTCGCCGC TCCTTTATTG CACAAGCCGA AGGAAAGGTT ACTACGTGAA CTCCCAAAGA</b>	3360
	<b>AACTTTTCTT CAGCACTAAC TTACTGAAGA TTTGCTG</b> <sub>gta</sub> <u>tgtcactttg tttttgctat</u>	3420
	<b>Sox6</b>	
	agtttaacac gtgtacattt gctatthtaa ggggtgctgta aacgcagttt aggactctta	3480
	agaagtgata tgtttthtaat catcatgttt aactcgcac gctcactgct cggttagaaa	3540
	aacgcgacgc gcagaactga cgttatagcg cttocagttt aattcatgaa gtttgtgttt	3600
	<i>Apa LI</i>	
	actaagtaaa gtgatattgg taaagttcgt gcac	3634

FIGURE 1 (Continued)

Additionally, there is sequence similarity between the zebrafish *tgfb3* promoter with their murine and rat orthologs, with an identity of 46% and 50%, respectively, and shared regulatory elements, such like glucocorticoid (GRE), androgen (ARE), c-Rel (NFkB), for TGF $\beta$  (Smad 3 and Fast 1) and for myogenic regulators (Myf 6, Mef 2C, and Prdm1a), among others (Figure 1B). Noticeably, in contrast with the murine promoter, the zebrafish BG promoter does not contain canonical MyoD or Myogenin binding sites. Nonetheless, it has six Sox6 binding elements, while the mouse *Tgfb3* promoter contains none.

### 2.3 | Zebrafish *tgfb3* promoter activity is enhanced during C2C12 myogenic differentiation

Murine *Tgfb3* is transcriptionally upregulated during skeletal muscle differentiation of murine C2C12 myofibroblasts.<sup>23</sup> To determine if zebrafish *tgfb3* promoter can mimic this response, we determined the activity of the p3.2 *tgfb3*:luc plasmid in C2C12 myoblasts induced to differentiate. Luciferase exhibited a 3.7-fold increase at day 4 of differentiation. In comparison, the murine *Tgfb3* promoter showed a 7.6-fold increase in this assay

(Figure 2). This difference may be explained by the fact that zebrafish promoter was tested in a heterologous murine myoblast cell line. A set of 5' nested deletions of the p3.2*tgfb3*:luc reporter was also assayed on days 0 and 4 of myogenic differentiation, along with the pGL3-basic and pGL3-promoter reporters as controls. As expected, the pGL3-basic activity was negligible both, prior (day 0) or after differentiation (day 4), while the pGL3-promoter reporter, containing the constitutive SV40 promoter, exhibited high activity at both 0 and 4 days, revealing that its strong activity is independent of the differentiation conditions (showing a 1.3-fold increase). Figure 2 also indicates that all zebrafish promoter nested deletions increased their transcriptional activity upon differentiation, and none of them seems to be uniquely responsible for the induction. The presence of Mef2, Myf6, Mef2C binding sites (black arrowheads in Figure 2) correlates with higher fold increases in luciferase activity of the constructs containing these sites. Nonetheless, even the promoter fragments that lack them ( $\Delta$ 1.2,  $\Delta$ 0.9, and  $\Delta$ 0.6), exhibit some degree of expression dependent on myogenic differentiation ( $\sim$ 2X fold increase). These latter deletions have Mef2 regulatory elements with lower MatInspector matrix similarity scores but also other binding sites for myogenic regulators that could be

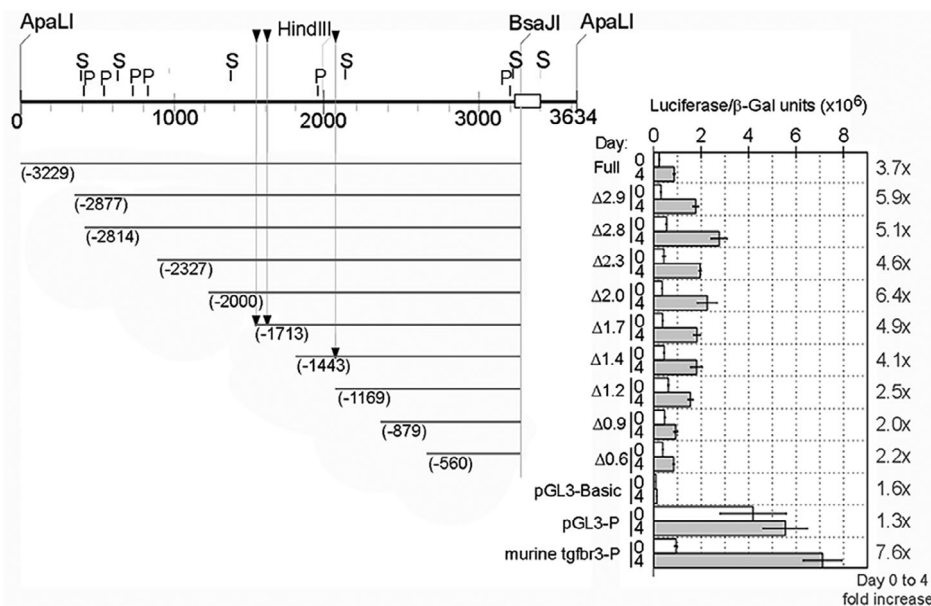


**FIGURE 2** Zebrafish *Tgfb3* promoter activity increases during myogenic differentiation. C2C12 myoblasts were transfected with the full-length zebrafish *Tgfb3* promoter reporter construct p3.2*tgfb3*:luc (full) or its 5' truncated deletion mutants (indicated as  $\Delta$ , with the kbp remaining in the plasmid), or with the murine BG promoter, or the pGL3 basic or pGL3 promoter negative or positive control vectors. Each one of these plasmids were co-transfected with a constant amount of a beta-galactosidase constitutive reporter. The cells were subjected to differentiation conditions and luciferase and galactosidase activities were determined. The beta-galactosidase-normalized luciferase activities obtained before (day 0) or after 4 days of differentiation are shown in the graph. The ratio of the normalized luciferase activity at day 4 over day 0 is indicated on the right margin of the graph as fold increase. Positions of the discussed myogenic responsive elements (arrowheads) and putative binding sites for Sox6 (S) and Prdm1a (P) are indicated.



responsible for remaining transcriptional activity. In summary, these results demonstrate that, like its murine counterpart, the zebrafish *tgfbr3* promoter is upregulated during the C2C12 myogenic differentiation, nonetheless, the main cis-regulatory elements responsible for this activation remain to be identified.

## 2.4 | Zebrafish *tgfbr3* promoter is active during development

To test if the cloned zebrafish promoter is active in vivo, we assembled a reporter plasmid that could be used for transient and stable transgenic expression. For that purpose, we employed the Tol2 kit<sup>24</sup> to recombine the 3.2 kb ApaLI-BsaJI fragment, the nls-tagged mCherry and the poly-adenylation sequences, and thus create the p3.2*tgfbr3*:nls-mCherry:polyA reporter plasmid (Figure 3A). Embryos injected with this construct at the one cell stage exhibited mosaic mCherry expression in the skeletal and cardiac muscle by around 48 hpf (Figure 3B,C), by the 72 hpf, the mCherry expression was stronger and included other organs such as the pronephric ducts and otic vesicle (Figure 3D,E), indicating that the 3.2 kbp ApaLI-BsaJI fragment has promoter activity in vivo and could be used to track the *Tgfbr3* expression during zebrafish development.

## 2.5 | Zebrafish *tgfbr3* promoter is turned on shortly before the start of somitogenesis

With the goal of obtaining fish that stably express the p3.2*tgfbr3*:nls-mCherry:polyA transgene, embryos were co-injected with p3.2*tgfbr3*:nls-mCherry:polyA plasmid together with the Tol2 mRNA and larvae expressing mCherry were grown to adulthood. Adults carrying the transgene in the germline were identified by crossing with wild-type fish. From 30 fish raised to adulthood, 6 of them (founder fish, F0) had progeny with mCherry expression. Two independent founders were mated with wild-type fish to obtain F1 establishing stable transgenic lines (Lines 3 and 6). Siblings from these lines had the same mCherry expression pattern (not shown), since line 3 had stronger mCherry fluorescence it was chosen for further experimentation and is here on referred to as *Tg(tgfbr3:nls-mCherry)*.

An initial observation with *Tg(tgfbr3:nls-mCherry)* was that mCherry was detected from single cell stage onward, when the fertilized oocytes came from a transgenic female, indicating maternal inheritance (Figure 4A). Furthermore, female transgenic adult fish accumulated *Tgfbr3* and mCherry proteins in their oocytes (not shown). On the other hand, when the embryos were obtained from crosses of transgenic males and wild-type females, embryos lacked the reporter at

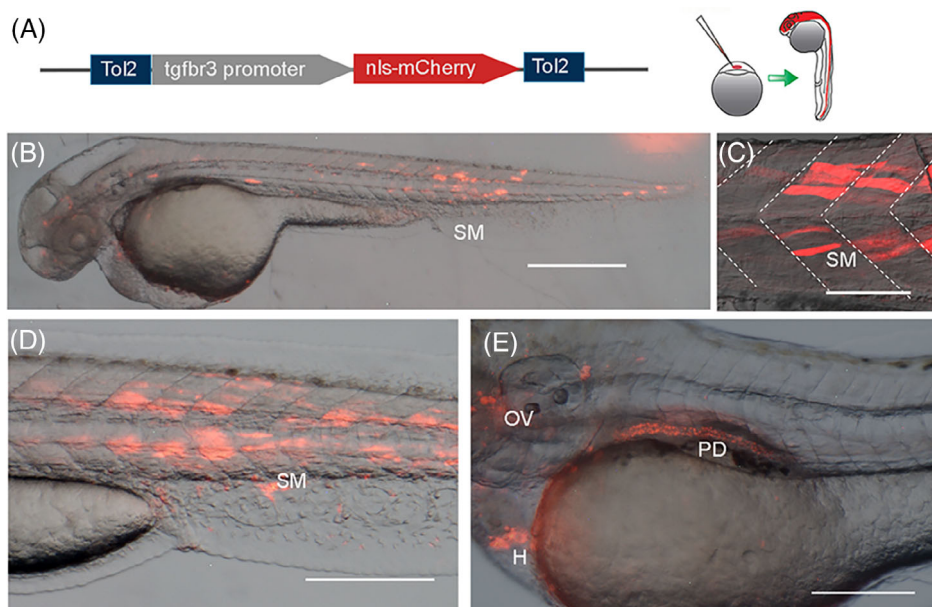


**FIGURE 3** *tgfbr3* promoter drives reporter expression during embryonic development. (A) p3.2*tgfbr3*:nls-mCherry:polyA reporter plasmid was injected in single cell zebrafish embryos, resulting in the mCherry mosaic expression at later stages. (B, C) 48 hpf embryos display mCherry in the head and skeletal muscle cells (SM) in somites resembling the aspect of superficial slow muscle fibers. (D, E) 72 hpf zebrafish embryos with reporter expression in skeletal muscle (SM), otic vesicle (OV), pronephric duct (PD), and heart (H). All images were acquired in a stereoscopic microscope Nikon SM1500. Scale bars: 400  $\mu$ m in (B); 50  $\mu$ m in (C, D); and 200  $\mu$ m in (E).

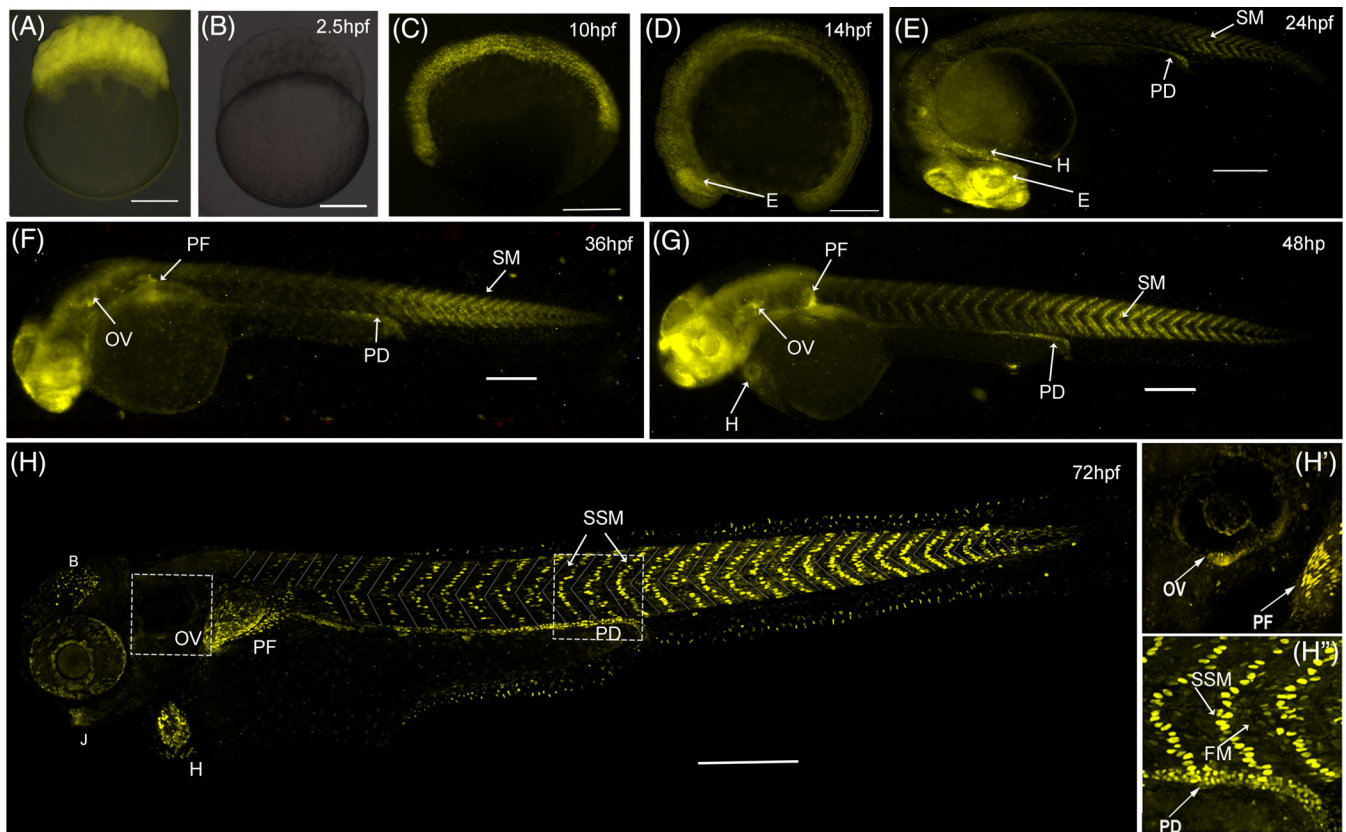


**FIGURE 4** mCherry expression begins just before somite formation. (A, B) mCherry fluorescence (shown in yellow) in 2 hpf zebrafish zygotes obtained from a wild-type fish crossed with a transgenic female (panel A) or transgenic male (panel B). (C–H) zygotic mCherry expression in zebrafish embryos obtained from crosses of transgenic males and wild-type females starts at 10 hpf (panel C). By the 14 hpf (panel D), mCherry is observed in the eye (E) and mesodermal tissue including the somites. At later stages (panels E–H), mCherry expression is clearly observed in the trunk superficial skeletal muscle (SSM), heart (H), pectoral fin (PF), otic vesicle (OV), pronephric duct (PD), jaw (J), and non-identified cells from the eye and brain (B). Inset H' shows the reporter expression in the OV and PF. Inset H'' shows mCherry in skeletal mononuclear muscle cells at the level of somites 14 to 16. Scale bars 200  $\mu$ m.

initial stages of development (Figure 4B). In this case, the mCherry fluorescence appears diffusely in mesodermal tissues at 10 hpf (Figure 4C) before the formation of the first somite. Importantly, this time of initial mCherry expression matches with the time of appearance of *tgfb3* mRNA as detected by RT-PCR.<sup>19</sup> By 14 hpf, mCherry is observed in the eye and mesoderm, including the somites (Figure 4D). At 24 hpf, the reporter expression starts to be confined to specific structures like heart, pronephric duct, eyes, and the somites where it adopts a chevron like arrangement (Figure 4E) which becomes very evident at later stages (Figure 4H). By 36 and 48 hpf, the otic vesicles and the pectoral fins present the reporter (Figure 4F,G) and by 72 hpf is also expressed in other head structures such as jaws and brain (Figure 4H,H', H''). Remarkably, the expression in somitic muscle resembles the characteristic pattern of the singly nucleated superficial slow-twitch muscle (SSM) fibers, although a fainter expression is also observed in fast twitch muscle multinucleated fibers (Figure 4H'' inset). A

more complete and detailed report on the patterns of *tgfb3* expression in other embryonic structures and times will be published elsewhere; here we focus on describing its expression in the somitic muscle, showing that the *tgfb3* reporter tracks presomitic adaxial cells during their radial migration to form SSM fibers.

## 2.6 | *Tg(tgfb3:nls-mCherry)* recapitulates *Tgfb3* protein expression in trunk skeletal muscle

To verify that the reporter expression occurs in tissues and structures expressing *Tgfb3* protein we performed an immunohistochemistry in whole embryos as well as sections of the trunk and tail. Both, *Tgfb3* and mCherry proteins were detected in the eye and somites at 14 hpf (Figure 5A,D), and otic vesicle, heart, and skeletal muscle at 24 hpf (Figure 5B–E). Noteworthy, in every structure and time shown in Figure 5A–F, the mCherry expression



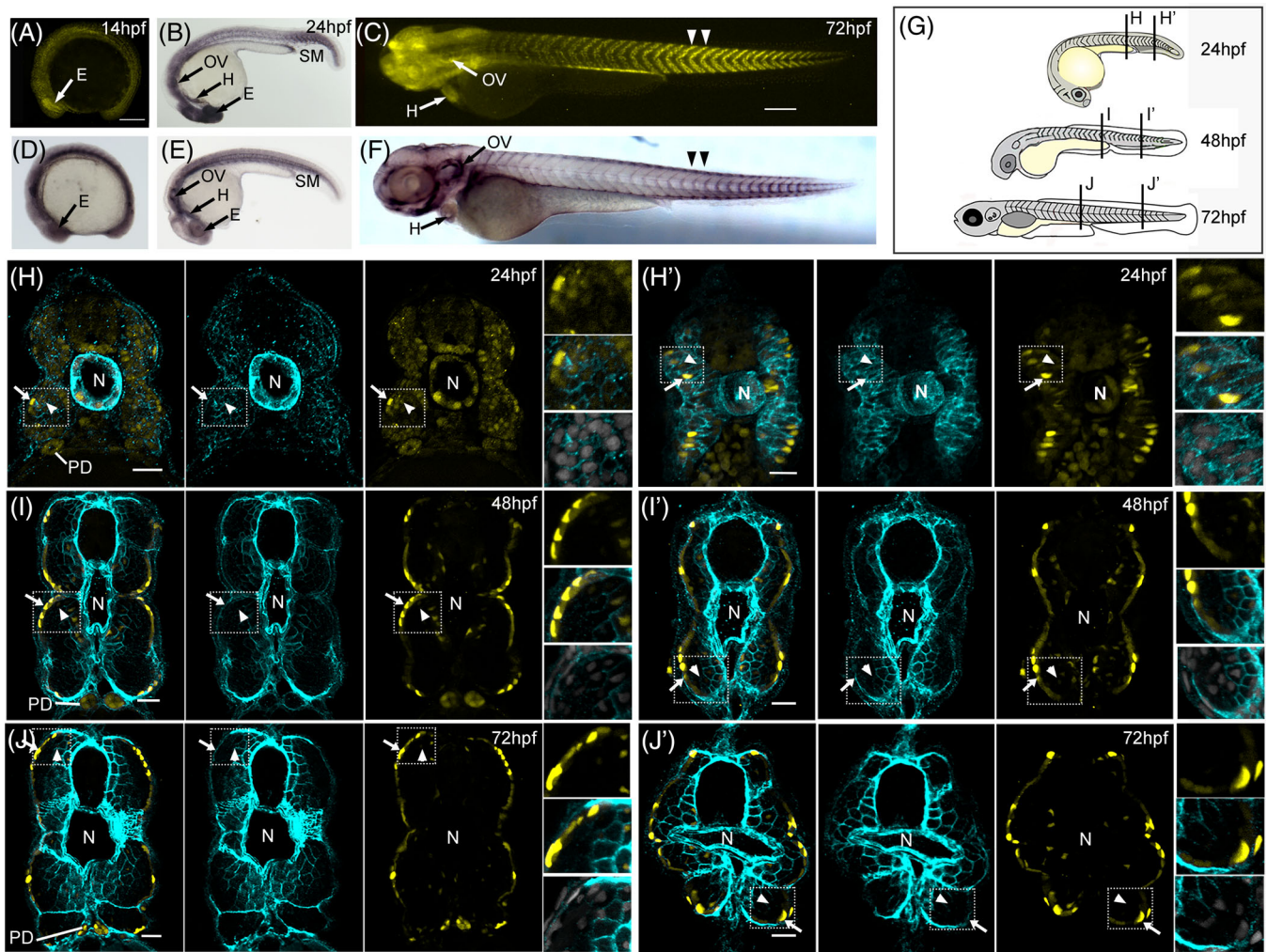


**FIGURE 5** *Tg(tgfb3:nls-mCherry)* recapitulates *tgfb3* expression in skeletal muscle lineage. (A–F) Lateral views of whole mounted embryos immunostained for *Tgfb3* (panels D–F) or mCherry protein (panel B); in panels A and C, the reporter mCherry fluorescence is shown. Panels D to F show *Tgfb3* protein expression in heart (H), otic vesicle (OV), eye (E), and skeletal muscle (SM). At 72 hpf, mCherry fluorescence and *Tgfb3* are higher in the posterior trunk somites (double arrowhead in C and F, respectively). Panels A to C show that mCherry expression matches with the co-receptor immunodetection at the indicated structures and time points. (H–J) The expression of *Tgfb3* protein (cyan) and mCherry (yellow) detected by fluorescent immunohistochemistry on transversal sections from the embryo regions and hpf indicated in the cartoon shown in panel G. White arrowheads indicate deep muscle fiber cells and white arrows show superficial muscle cells with mCherry and protein expression in the somitic skeletal muscle. The insets also show the expression of *Tgfb3* and mCherry protein in skeletal muscle cells, Hoechst staining all the nuclei (light gray). Notochord (N) and pronephric duct (PD) position and *Tgfb3* expression are also indicated. Scale bars 50  $\mu\text{m}$ .

matched the co-receptor immunodetection. We observed reproducibly that mCherry and *Tgfb3* levels in posterior end somites are higher than in the anterior ones; Figure 5C,F are a representative 72 hpf example (double arrowhead).

Immunofluorescence on histological sections revealed that *Tgfb3* protein is expressed in muscle cells of the deep and superficial layers of the somitic muscle, being higher in the superficial muscle fibers (Figure 5H–J). The appearance, arrangement, and large size of these single-nucleated fibers suggested that they corresponded to SSM fibers. Additionally, in these sections *Tgfb3* and the

reporter proteins were detected in the notochord, pronephric ducts (Figure 5H–J).

At 24 hpf, *Tgfb3* and mCherry were expressed in every somitic cell (Figure 5H) with mCherry at higher intensity in the nuclei of the superficial muscle fibers (white arrows and insets in 5H). At 48 and 72 hpf, *Tgfb3* and mCherry keep being expressed in the skeletal muscle fibers but with higher intensity in superficial ones (compare white arrows and arrowheads and insets in Figure 5I,J). Interesting to note, the muscle fibers surrounding the neural tube and notochord keep expressing *Tgfb3* protein and mCherry at these development times (Figure 5H–J).

## 2.7 | *tgfbr3* promoter is transcriptionally active in presomitic adaxial cells and SSM fibers

To verify if *tgfbr3* reporter preferentially labels SSM cells and its precursors, the adaxial cells, we performed an immunohistochemistry in flat mounted specimens using the streptavidin amplification system (Figure 6A,B). At

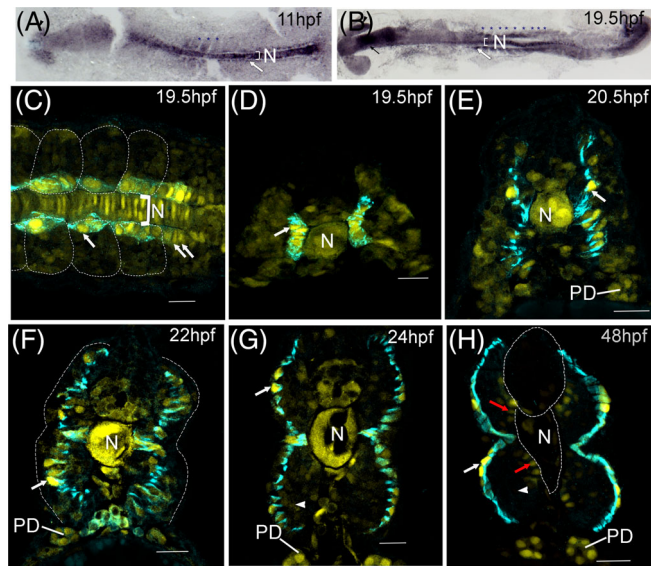


**FIGURE 6** *tgfbr3* promoter is upregulated in slow muscle and marks adaxial cells during their radial migration. (A, B) Immunohistochemistry for mCherry in flat mounted transgenic zebrafish embryos. High mCherry expression is detected in the notochord (N), in somitic mesoderm (indicated by blue asterisks) with higher signal in adaxial cells (white arrows) from presomitic and somitic mesoderm at 3 somite (11 hpf) and 19 somite stages (19.5 hpf). Expression is also observed in the eye (black arrowhead) and head (black arrow). (C-H) immunofluorescent staining of mCherry (yellow) and F59 (cyan). Dorsal view (panel C) of an embryo at 19.5 hpf (somites 16-19). Adaxial cells were labeled with F59 (cyan), mCherry is observed with higher fluorescence in the nuclei of adaxial cells from the somitic mesoderm (white arrow) and adaxial cells from presomitic mesoderm (double white arrows). Cells in the notochord (N) express high levels of mCherry. Transverse sections (panels D-H) in the caudal trunk (somites 14-17) show mCherry in the nuclei of adaxial cells (white arrows), which are revealed by the F59 staining (cyan). This monoclonal antibody marks the adaxial cells during their radial migration from 19.5 to 24 hpf (panels D-G) all the way to the somite surface where they become slow fibers (panel H). mCherry expression in notochord (N) and somitic fast muscle decreases gradually (white arrowheads in panels G and H), except in the fast fibers in contact with the notochord and neural tube (red arrows), while in the nuclei of superficial slow muscle fibers the mCherry expression increases (white arrows). The expression in pronephric ducts (PD) increases as development proceeds. In dorsal views, embryos are oriented with head to the left. Scale bars, 20  $\mu$ m.

11 and 19 hpf, the mCherry reporter can be detected in the notochord and in the cells adjacent to the notochord from somitic and presomitic mesoderm in a characteristic pattern described before for the adaxial cells.<sup>25</sup> To confirm the identity of adaxial cells we employed the F59 monoclonal antibody, specific for myosin heavy chains, that labels slow muscle cells strongly and has been used before to track adaxial cell migration.<sup>26</sup> Immunohistochemistry of histological sections of embryos from 19.5 to 48 hpf at somites 14 to 17 clearly shows the radial migration of the adaxial cells from the surroundings of the notochord to the surface of the somite. During this migration, the nuclei of adaxial cells were labeled with high intensity with mCherry (Figure 6D-H). At 24 and 48 hpf, when the adaxial cells have completed their migration, the cells with the highest nuclear level of mCherry are also strongly immunoreactive to F59 (Figure 6G,H). As expected, the reporter fluorescence also reveals cells in the pronephric ducts as well as cells surrounding the notochord and the neural tube in these sections. On the other hand, the fainter mCherry signal of the internal somitic fast muscle fibers indicates a preferential expression of *Tgfbr3* in slow over fast muscle cells even at their initial developmental origin. In summary, these immunofluorescent co-detection experiments with the F59 antibody and the mCherry fluorescence indicate that *tgfbr3* reporter strongly labels the nuclei of adaxial cells and tracks them during their journey to the somitic surface, where they become slow-twitch muscle fibers at later stages of development (Figure 6D-H).

## 2.8 | *tgfbr3* promoter transcriptional activity is higher in the posterior somites of the zebrafish larvae

Figures 4H and 5C are examples of an intriguing and reproducible observation, namely, that mCherry appears in the SSM cells with higher brightness in the posterior somites of the tail than in those located more anteriorly in the trunk. It can be observed after 24 hpf and becomes very evident by 72 hpf, when the mCherry fluorescence is higher at the most posterior somites, gradually increasing as they get closer to the tail (Figures 4F-H and 5C). Importantly, this is also evident and reproducible when the *Tgfbr3* protein is observed, as shown in Figure 5F, indicating that *tgfbr3* expression is subjected to an antero-posterior (A-P) axis gradient. Figure 7B shows a representative confocal image of 72 hpf larvae evidencing this increase in the intensity fluorescence along the A-P axis.

To determine if *tgfbr3* reporter is indeed activated differentially in an A-P axis gradient, we used 72 hpf



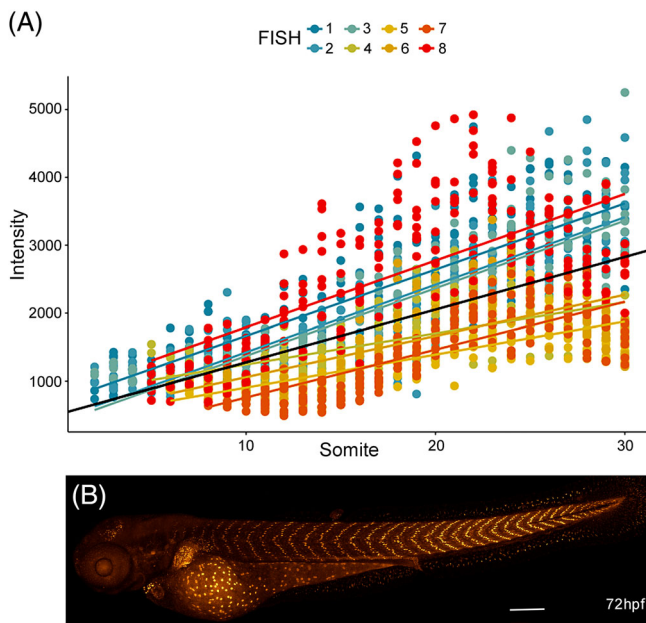


**FIGURE 7** *tgfr3* promoter has higher activity in slow muscle fibers of the posterior trunk somites. (A) The linear regression shows an increase in the normalized mCherry fluorescence intensity with respect to somite location. Each point in the plot represents the value obtained for single nuclei after normalizing with Hoechst staining as described in the text. Intensity fluorescence from eight nuclei were measure per somite, in eight different embryos at 72 hpf. Individual slopes are color-coded, and the overall regression is in black. (B) Representative image of the A-P gradient expression gradient in 72 hpf Tg(*tgfr3:nls-mCherry*) embryo.

confocal images like those in Figure 7B to quantify mCherry expression from somites 1 to 30. Eight whole embryos and eight nuclei per somite were processed as follows. Image acquisition was done using a confocal microscope. To eliminate the florescence variation due to vertical position (z-axis), we stained and quantified the fluorescence intensity of nuclear-Hoechst and used these values to calculate fluorescence change associated with z separately for each fish. This change was then subtracted from the mCherry intensity to obtain a normalized value of mCherry fluorescence intensity. Plotting this against somite number (Figure 7A) revealed that mCherry intensity increased toward the more posterior somites at a rate that was similar along each somite in every fish. A linear regression analysis (linear mixed-effects models in R using the lme4 package<sup>27</sup>) indicated that the rate of increase was statistically significant and had an average value of 0.21 units per somite ( $P < .001$ ), representing a total 6.3-fold increase from somite 1 to 30. A linear mixed-effects model was used instead of the ordinary regression because it fits coefficients for each individual as well as the overall trend, and thus, can account for

individual variability. The conclusion from this analysis is that, in the Tg(*tgfr3:nls-mCherry*) transgenic zebrafish, the mCherry fluorescence intensity increases linearly from head to tail somites, in 0.21-fold increments from one somite to the next along the A-P axis.

### 3 | DISCUSSION

In this work, we report the identification and cloning of the zebrafish *tgfr3* gene promoter, which was used to create a mCherry reporter that demonstrates differential *tgfr3* muscle lineage expression, especially in somitic SSM muscle fibers and their precursors, the adaxial cells. To our knowledge, this is the first report of a non-mammalian *tgfr3* promoter and its somitic muscle lineage specificity. Ensemble (ENSDART00000167482.1) and Genbank (*tgfr3*) annotations (Figure 8A,B), report two different predicted primary transcripts for betaglycan, the former includes our experimentally determined exon 1, and the latter does not. Aside from this difference, both primary transcripts are identical and show an exon-intron distribution that is comparable to the mammalian *Tgfr3* orthologs. Our assignments of *tgfr3* exon 1 and promoter are based on experimental evidence and agree with ENSDART00000167482.1. This is further supported by bioinformatic analysis. Namely, the H3K4me3 signatures at the ZF genome, which are considered epigenomic markers of transcriptional initiation sites,<sup>28</sup> revealed a strong peak just around our experimentally determined exon 1, confirming that the ENSDART00000167482.1 is the bona fide *tgfr3* full transcript (Figure 8A,B).

Analysis of the *tgfr3* promoter sequence indicates that it is a TATA-less promoter containing a SP1 site that may function as transcription initiation site as in the rat ortholog.<sup>22</sup> Alignment comparison with its rat and mouse orthologs shows that zebrafish *tgfr3* promoter shares putative binding sites for transcriptional regulators, including those that may confer transcriptional activation during the myogenic process. In accordance with its muscle lineage expression, the murine *Tgfr3* promoter is transcriptionally upregulated during C2C12 myoblast differentiation.<sup>23</sup> The 3.2 kb fragment from the zebrafish *tgfr3* gene that we are now reporting is also transcriptionally induced during the C2C12 myoblast differentiation. This indicates that its nucleotide sequence conservation with respect to its vertebrate orthologs is due to functional conservation.

These similarities are revealed by the activation of our reporter during the C2C12 differentiation assay. Although the murine promoter did better in this assay, the zebrafish promoter fared well enough, despite the facts that it was tested in mouse myoblasts, and that it



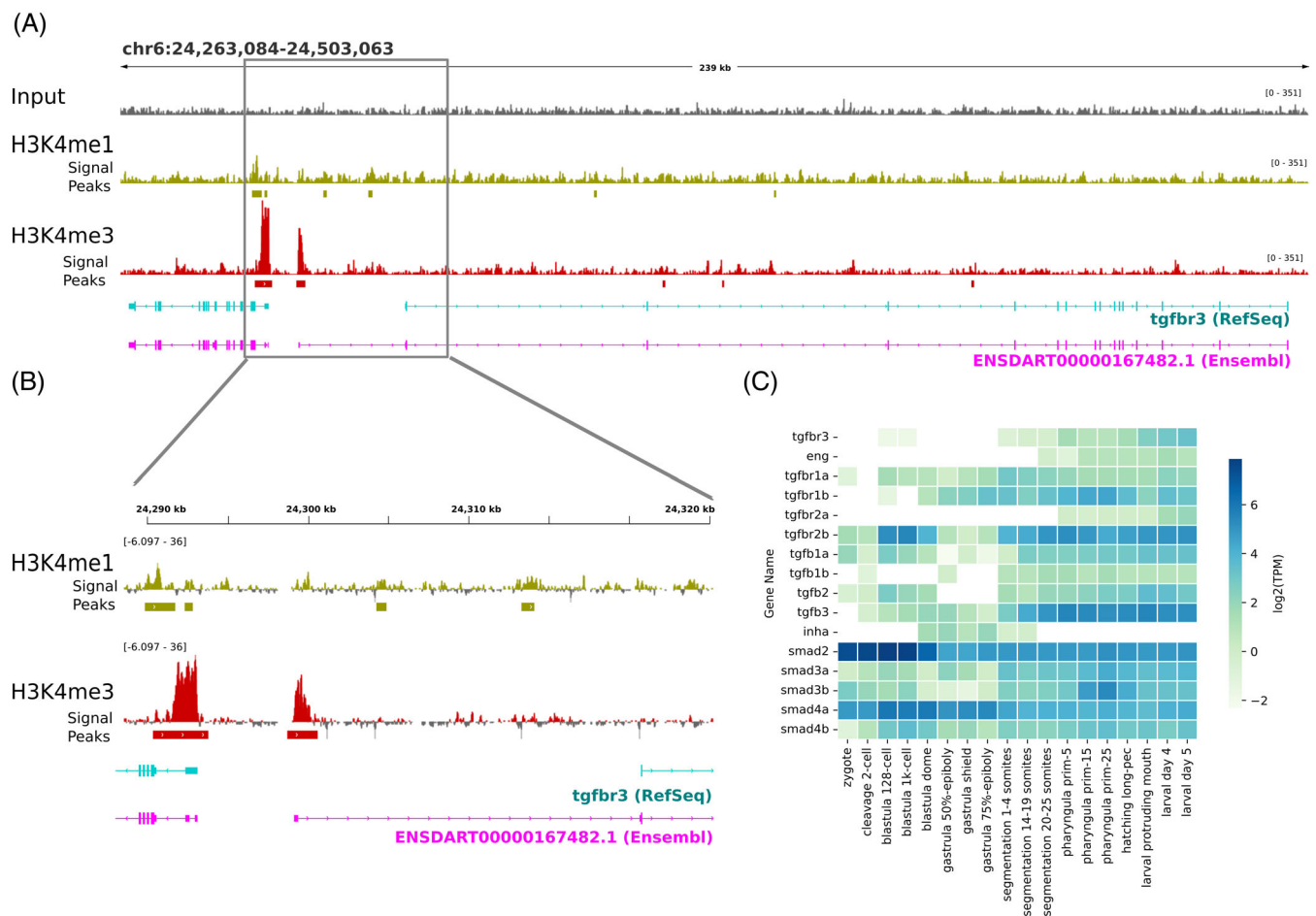


**FIGURE 8** Histone 3 epigenetic markers around *tgbr3* exon 1 and gene expression analysis of components of the TGF $\beta$  canonical pathway. (A, B) Visualization of heterochromatin H3K4me1 and H3K4me3 marks over zebrafish betaglycan locus indicates strong H3K4me3 signals around the Ensembl predicted primary transcript. (C) Expression of genes encoding components of TGF $\beta$  canonical pathway during the indicated zebrafish developmental stages. Data were obtained from raw data repositories (Expression Atlas <https://www.ebi.ac.uk/gxa/experiments/E-ERAD-475/Results>) as described in the methods.

does not contain canonical MyoD or myogenin sites as the murine promoter does. Other elements in the promoter sequence, which could not be mapped by our initial deletion analysis shown in Figure 2, might be responsible for the myogenic induction. Thus, *tgfb3* zebrafish promoter expression in muscle was expected and confirmed; however, its clear preference for the adaxial cells and their descendants, the SSM cells, was surprising.

Skeletal muscle patterning and lineage specification is conserved among vertebrates. The muscle fibers differentiate into two main subtypes, slow- and fast-twitch muscle, distinguishable by their metabolic properties and motoneuron innervation. This muscle lineage differentiation has been extensively studied in zebrafish due to the feasibility of distinguishing slow-twitch from their fast-twitch fibers counterparts.<sup>25,26</sup> Slow twitch precursors can be easily distinguished from fast twitch because they

remain mononucleated during embryonic and larval stages.<sup>29</sup> Multinucleated fast muscle fibers preferentially use glycolytic pathways, while mononucleated slow fibers rely on oxidative pathways.<sup>30</sup> Many studies have described the origins and development of these lineages and have concluded that after its muscle commitment, the presomitic mesoderm adjacent to the notochord, the adaxial cells, differentiate into the SSM.<sup>31-33</sup> The specification of the adaxial cells and their stereotypic migration from the sides of the notochord to their final position on the surface of the myotome have been attributed to a selective transcriptional regulation in which Hedgehog signaling activates *Prdm1a* specifically in the adaxial cells.<sup>32,34,35</sup> *Prdm1a*, also known as *Blimp1*, is a transcriptional repressor of the fast-twitch muscle program genes. Additionally, *Prdm1a* also represses *Sox6*, which functions as a repressor of the slow-twitch muscle program. This double repression results in the blocking of the fast-

twitch differentiation simultaneously with the unblocking of the slow-twitch differentiation program.<sup>36</sup> Interestingly, the zebrafish *tgfb3* promoter contains putative binding sites for both Sox6 and Prdm1a, suggesting that its activity is unconstrained in the adaxial cells. Determining which of these putative sites is more relevant than the other for myodifferentiation will certainly shed light into the complex expression pattern of *tgfb3* and the regulation of somitic muscle lineages in the zebrafish.

In zebrafish, the adaxial cells remain adjacent to the notochord before somite formation, where they are specified in response to Sonic Hedgehog and characteristically express Prdm1a and Prox1 transcription factors (TFs) as well as the slow isoform of myosin heavy chain.<sup>33,37,38</sup> Shortly after somite formation, adaxial cells elongate to cover the length of the entire somite and migrate radially away from the notochord to form a superficial layer of mononucleated slow muscle fibers that surrounds the somite, this migration process takes approximately 5 hours. Our data, as illustrated in Figure 6, shows that *tgfb3* promoter is specifically active in the adaxial cells and tracks their migration into becoming SSM. At later stages, the cells in immediate contact with the notochord and the neural tube continue to express mCherry and Tgfb3 protein which indicates responsiveness to a signal coming from these structures. However, we observed that the mCherry fluorescence decrease in the notochord after 24 hpf (Figures 5 and 6) was not followed by a similar decrease for *tgfb3* gene product. This may indicate that the Tgfb3 protein is either more stable in these cells or that the native gene continues being expressed and the promoter sequence studied here does not have the regulatory sites for notochord expression at posterior stages.

The 3260 bp-long ApaLI-BsaJI fragment we have used in the *Tg(tgfb3:nls-mCherry)* transgenic zebrafish contains enough information to recapitulate the endogenous gene expression in the trunk skeletal muscle lineages and in other embryonic structures (Figure 5). A comparison with available mRNA sequencing developmental profiles agrees with our finding that the *tgfb3:nls-mCherry* is activated at the initiation of somitogenesis (Figure 8C).<sup>39</sup> The faint expression of *tgfb3* reported at blastula stages, just before the zygotic genome activation and that is not apparent in our transgenic fish, could be due to maternal contribution. Because of the complexity of the maternal-to-zygotic transition in the zebrafish,<sup>40</sup> we cannot rule out the possibility of a true zygotic expression that is missed by the promoter sequences we have studied.

In all vertebrates, somites develop from anterior to posterior along the embryonic axis in response to signals such as retinoic acid and Wnt.<sup>41</sup> Nord and colleagues

reported a muscle regionalization along the A-P axis of zebrafish embryo. They showed that different isoforms of the myosin heavy chain sarcomeric proteins are expressed from head to tail and define specific muscle domains.<sup>42</sup> Our data, illustrated in Figure 7, document that *tgfb3* promoter activity displays an A-P gradient expression which could be important for the specific localization or activity of any of its many ligands.

The functional relevance of expressing *tgfb3* in the SSM is an open question. We have demonstrated that in the null *tgfb3* zebrafish there is a delay in the mineralization of the chordocentra, the vertebrae primordia, and have proposed that this delay is due to the absence of TGF $\beta$  signaling enhancement, a function that has been well documented for this co-receptor.<sup>19</sup> However, given the many biochemical activities that have been found in vitro for Tgfb3, it is hard to propose a specific role for its selective expression in the adaxial cells and the SSM, particularly, given its A-P gradient expression documented in Figure 7. It is tempting to hypothesize that *tgfb3* expression is not only responding to a morphogen gradient but may help creating such a gradient. It has been proposed that secreted morphogens create gradients of concentration determined by their diffusion rates. However, free diffusion of morphogens may be “hindered” by interactions with molecules in the extracellular matrix.<sup>43,44</sup> The animal-vegetal axis gradient of FGF8a has been documented and is proposed to be created due to hindered-diffusion by heparan-sulfate containing proteoglycans.<sup>45</sup> The fact that Tgfb3 is a heparan-sulfate proteoglycan that exists as an integral membrane protein of which the extracellular domains can be shed as a soluble receptor, invites to the speculation that it plays a role in hindering the diffusion of still unidentified, morphogens during development. Finally, a comparison of the abundance of betaglycan mRNA with the other genes coding for components of the canonical TGF $\beta$  signaling pathway (Figure 8C) reveals that the minimal set of components (ligands, receptors, and Smads) is present through all the embryonic stages, while the co-receptors endoglin (*eng*) and betaglycan (*tgfb3*) need not to be present during early embryogenesis. Interesting to mention is the observation that TGF $\beta$ 2 and inhibins (*inha*), both selective betaglycan ligands, are already present before *tgfb3* expression. This is in line with the ideas that *tgfb3* roles are more diverse than being just the TGF $\beta$ 2 equalizer or that of another co-receptor that may mediate inhibin actions.<sup>46</sup> As it is common with betaglycan, the present study has poised more questions than it has answered. However, the availability of zebrafish *tgfb3* promoter shall provide the tools to delve into these new questions.

## 4 | EXPERIMENTAL PROCEDURES

All restriction enzymes for cloning were obtained from New England Biolabs. TOPO TA-cloning kit for PCR was purchased from Invitrogen. Kits for in vitro transcription AmpliCap SP6 high yield message maker kit and A-plus poly (A) polymerase tailing kit both were from Cell Script. Zebrafish BAC clone DKEY 197A14 was purchased from SourceBiosciences. pGL3B vector, luciferase assay and Erase a Base kits were from Promega, pCMV- $\beta$ Gal and pGL3P vectors were kindly provided from Dr Felix Recillas Targa (Instituto de Fisiología Celular, UNAM) and Dr Angel Zarain (Facultad de Medicina, UNAM). Tol2 kit vectors were kindly provided by Dr Kawakami. All cell culture media were from Gibco BRL, lipofectamine 2000 from Thermofisher, and cytosine- $\beta$ -D-arabinofuranoside from Sigma Aldrich.

### 4.1 | Zebrafish maintenance and care

Wild-type zebrafish (*Danio rerio*) are crosses of genomic backgrounds TAB 14 vs Wik (T/W), first strain kindly provided by Professor Nancy Hopkins at Massachusetts Institute of Technology and the latter obtained from Zebrafish International Resource Center. Adult zebrafish were maintained according to standard procedures.<sup>47</sup> Embryos were staged according to Kimmel by hpf or somitic stage of development.<sup>48</sup>

### 4.2 | Zebrafish *tgfb3* promoter cloning

The strategy to identify the putative exon I for zebrafish *tgfb3* using the EST clone EB978660 and RT-PCR is described in the text. To perform RT-PCR, total RNA from at least twenty 48 hpf embryos was obtained with Trizol reagent (Invitrogen) according to manufacturer instructions, first strand cDNA was synthesized with oligo (dT) and M-MLV reverse transcriptase from Invitrogen, PCR was performed using primer 3.20 (ccgtggcgtttgtcgcggtattaat) and primer 3.13-(cggtgatgagcccaattaagcaga) or primer 3.15 (gcatcaaaggagggaatgactggt).

To clone the region upstream of exon 1, a 3624 bp (ApaLI-ApaLI) fragment was isolated from the commercially available zebrafish BAC clone DKEY-197A14 (SourceBiosciences). The BAC DNA was cut with *ApaLI*, filled in with Klenow fragment and cloned at the *SmaI* site of the pGL3B vector. This plasmid was cut with *BsaJI*, filled-in with Klenow, and with *SacI* and the resulting 3.2 kbp insert was subcloned at the *SacI-SmaI* sites of pGL3B vector to obtain the p3.2*tgfb3*:luc plasmid. The nested 5' to 3' deletions used in Figure 2 were

generated with Erase-a-base system kit (Promega) according to manufacturer instructions.

To create the p3.2*tgfb3*:nls-mCherry:polyA reporter plasmid we used the gateway system and the Tol2 kit vectors to generate the plasmid for transposon mediated transgenesis (Kwan et al. 2007). The 5' entry clones (p5E) containing BG promoter were generated by subcloning the *KpnI/XhoI* fragment (excised from p3.2*tgfb3*:luc) into the p5E-MS2 tol2 kit vector to obtain the 5' entry vector, which along with pME-nls-mCherry and p3E-polyA and pDest-Tol2pA2 were used at equimolar ratio for gateway LR reaction to generate p3.2*tgfb3*:nls-mCherry:polyA.

### 4.3 | Promoter nucleotide sequence analysis

Promoter sequence was analyzed using MatInspector<sup>21</sup> to identify putative TF binding sites. TF binding sites with a minimum matrix similarity value of 0.80 were considered for comparison with rat and mouse orthologous sequences.

### 4.4 | Cell culture promoter activity assay

Promoter activity was tested in zebrafish ZF4 fibroblast.<sup>20</sup> Cells were seeded on 100 mm plates at a density of 10 000 cells/cm<sup>2</sup> and transfected 24 hours later with 3  $\mu$ g of total DNA containing p3.2zBG-Prom, or pGL3B (the empty vector) plus pCMV- $\beta$ GAL. Cells were harvested 2 days after transfection and the luciferase activity was measure in samples containing 20  $\mu$ g of protein. All data were normalized to  $\beta$ GAL activity. Luciferase activity was measured according to manufacturer protocol (Promega),  $\beta$ -galactosidase was determine as described before.<sup>49,50</sup>

To quantify transcriptional activity during murine C2C12 myoblast differentiation, cells were seeded at 58 000 cells/well, on six well-plates and lipofected after 48 hours with 3  $\mu$ g of total DNA containing pGL3B, 3.2*tgfb3*3P or any of its deleted versions plus 10% pCMV- $\beta$ Gal. After lipofection, cells were culture in DMEMF12/10% SFB (day 0). The next day, myoblasts were induced to differentiate by culturing cells in mitogen free media (DMEMF12/5% Horse serum) with cytosine- $\beta$ -D-arabinofuranoside at 1 mM final concentration, thereafter media was changed every day. Cells were harvest at day 0 or 4, and luciferase activity was measured (Promega) according to manufacturer protocol,  $\beta$ -galactosidase was determined after 2 hours of incubation.

## 4.5 | Obtaining and breeding of transgenic zebrafish line

In vitro transcription was done with AmpliCap SP6 and A-plus poly(A) tailing kit. Then, 30 pM of p3.2*tgfbr3*:nls-mCherry:polyA plasmid was injected together with 20 pM of transposase RNA at 1 cell stage embryo, 30 injected zebrafish embryos were raised to adulthood. Injected and transgenic embryo were observed to determine sites of transcriptional activity by expression of mCherry fluorescent protein during zebrafish development. A group of 30 founder fish (F0) were grown to adulthood and screened at 3 to 4 months to identify fish carrying the transgenic construct in germline.

To maintain the transgenic zebrafish lines 3 and 6, only the embryos with higher mCherry expression were selected. For this purpose, only the embryos with expression visually detected in five somites of development were raised to adulthood. From the six zebrafish founders, two independent lines with the highest mCherry expression (lines 3 and 6) were mated with wild-type zebrafish to obtain F1. For subsequent maintenance of the transgenic line, F2 and F3 were obtained only after mating males and females with the highest mCherry expression among their siblings, this was important because the expression of mCherry at initial stages of development is low and otherwise difficult to detect. For the experiments, we used embryos from F3 or F4.

## 4.6 | Immunofluorescence and immunohistochemistry

In all the experiments, we used embryos from F2 or F3. These embryos were treated with phenylthiourea 0.003% at 20 hpf to avoid pigmentation, dechorionated, and fixed with PFA 4% at the appropriate stage. Embryos were dehydrated at RT in methanol 25%, 50%, and 100%, 5 minutes for each change. Embryos were incubated in PBST/15% goat serum/2% BSA for 2 hours at RT or overnight at 4°C to block unspecific signal of antibodies. Concentrations and conditions for primary antibodies: BG031 rabbit polyclonal specific for zebrafish TGFBR3 (1:1000),<sup>18</sup> mouse monoclonal IgG mCherry (1:500, Clontech), mouse monoclonal IgG1 F59 specific for slow muscle (1:10, DSHB) were incubated in PBST/5% GS/2% BSA for 2 hours at RT or overnight at 4°C. Secondary antibodies (Alexa 488 or Alexa 594) were incubated in PBST/5% GS/2% BSA for 1 hour at RT. Embryos were washed and mounted for image acquisition in low melting point agarose 1%.

For immunohistochemistry of tissue sections, the same concentrations of antibodies were used. The

primary antibodies were incubated for 2 hours at RT or overnight at 4°C, secondary antibodies were incubated for 1 hour. The slides were washed and mounted in Vectashield (VectorLabs). For tissue sections, the embryos were embedded in PBS/15% sucrose/7.5% gelatin and sectioned in a Leica cryostat at 16 or 20  $\mu$ m.

Images were acquired with stereomicroscope NIKON SMZ1500. NIS elements v4.1 software and DS-Fi1 camera both from NIKON were used to acquire images. Confocal microscopy used microscope LS800 with Zeiss Zen Blue 2.3 software and Plan-Apochromat  $\times$ 40/1.3 oil DIC(UV) VIS-IR M27 objective.

## 4.7 | *tgfbr3* promoter expression and quantification at A-P axis

To analyze *tgfbr3* promoter expression levels in the A-P axis we fixed *Tg(tgfbr3:mCherry)* transgenic zebrafishes at 72 hpf with PFA 4% overnight, washed five times at RT in PBST 0.1%. The embryos were permeabilized with PBST 0.5% overnight in rotation at 4°C and stained with Hoechst 33 258 (ThermoFisher) in PBST 0.3% overnight at 4°C. The embryos were washed three times with PBST 0.1% at RT and mounted for image acquisition in low melting point agarose 0.5%.

Imaging of whole embryos was done in an LSM800 Zeiss confocal microscope, using a Plan-Apochromat  $\times$ 20/0.8 M27 objective. Tile-imaging mode of a z stack was set and 16 bit images were acquired every 5  $\mu$ m. The same laser power was set for all the experiments ( $n = 8$ ). All image intensity processing was done using Multi Measure plugin (FIJI). Briefly, for image analysis we separated the images acquired on different channels (red for nuclear mCherry and blue for nuclear Hoechst 33258). On the red and blue channels, we measured the fluorescence intensity for eight nuclei in each somite from 1 to 30. The measurements were only registered on one focal plane for each nucleus. Specific ROI coordinates were assigned to each nucleus. In this way, we generated a map of coordinates used to measure the fluorescence intensity in blue channel. Then, we used these coordinates to obtain the same information on the red channel. The statistical analysis consisting of linear mixed-effects models, explained in Section 2, was performed in R using the lmer package<sup>27</sup>.

## 4.8 | Gene expression visualization

The gene expression of zebrafish transcripts was obtained from the data deposited by White et al. in the Expression Atlas repository.<sup>39</sup> The Transcript Per Million (TPM) file



was downloaded and the log<sub>2</sub>(TPM) expression levels from selected genes were visualized using ad hoc Python scripts.

## 4.9 | Chip seq visualization

To visualize heterochromatin related mark over loci of interest we used previously published data GEO accession number: GSE20600, specifically runs SRR122214 for H3K4me1 ChIP-Seq, SRR122215 H3K4me3 ChIP-Seq and SRR122216 as an input control. Raw data were aligned into danRer10 genome assembly using Bowtie 2 (Version 2.5.0 + galaxy0) with default parameters,<sup>51</sup> BAM files were then used to get BigWig files using bamCoverage<sup>52</sup> (Galaxy Version 3.5.1.0.0) with ×1 normalization using an effective genome size of 1 400 000 000, and a bin size of 1. Peaks were obtained using findPeaks tool of the Homer suite (version 4.11)<sup>53</sup> under default parameters using Input sample as control.

### AUTHOR CONTRIBUTIONS

**Lizbeth Ramírez-Vidal:** Conceptualization (equal); data curation (equal); formal analysis (equal); investigation (equal); writing – original draft (supporting); writing – review and editing (supporting). **Tonatiuh Molina-Villa:** Conceptualization (equal); investigation (equal); writing – review and editing (supporting). **Valentin Mendoza:** Investigation (supporting); project administration (lead); writing – review and editing (supporting). **Carlos Alberto Peralta-Álvarez:** Formal analysis (equal). **Augusto Cesar Poot-Hernández:** Data curation (equal); formal analysis (equal). **Dobromir Dotov:** Formal analysis (supporting); software (supporting); writing – review and editing (supporting). **Fernando López-Casillas:** Conceptualization (lead); formal analysis (equal); funding acquisition (lead); investigation (equal); methodology (equal); project administration (supporting); supervision (lead); writing – original draft (lead); writing – review and editing (lead).

### ACKNOWLEDGMENTS

The authors gratefully acknowledge the technical assistance of Gilberto Morales (Fish care and maintenance), Ruth Rincón Heredia, and Abraham Rosas Arellano (Microscopy Unit, IFC-UNAM), Sandra Daniela Rodríguez Montaña (Histology Unit, IFC-UNAM), Maria Guadalupe Codiz, Minerva Mora, and Laura Ongay (Molecular Biology Unit, IFC-UNAM). The authors are especially thankful to Dr Diana Escalante-Alcalde for the critical reading of the manuscript and her continuous advice during this work. Work at F.L.-C.'s lab is supported by grants 254046 (Conacyt) and IN204916,

IN204620 (PAPIIT-UNAM). L.R.-V. was supported by a Conacyt Graduate Scholarship (CVU 350628).

### ORCID

Fernando López-Casillas  <https://orcid.org/0000-0002-3689-1824>

### REFERENCES

- López-Casillas F, Wrana JL, Massague J. Betaglycan presents ligand to the TGFβ signaling receptor. *Cell*. 1993;73:1435-1444.
- Bernard DJ, Smith CL, Brule E. A tale of two proteins: betaglycan, IGSF1, and the continuing search for the inhibin B receptor. *Trends Endocrinol Metab*. 2020;31(1):37-45. doi:10.1016/j.tem.2019.08.014
- Lewis KA, Gray PC, Blount AL, et al. Betaglycan binds inhibin and can mediate functional antagonism of activin signalling. *Nature*. 2000;404:411-414.
- Velasco-Loyden G, Arribas J, Lopez-Casillas F. The shedding of betaglycan is regulated by pervanadate and mediated by membrane type matrix metalloproteinase-1. *J Biol Chem*. 2004;279(9):7721-7733. doi:10.1074/jbc.M306499200
- Arribas J, Lopez-Casillas F, Massague J. Role of the juxtamembrane domains of the transforming growth factor-α precursor and the beta-amyloid precursor protein in regulated ectodomain shedding. *J Biol Chem*. 1997;272(27):17160-17165. doi:10.1074/jbc.272.27.17160
- Andres JL, Stanley K, Cheifetz S, Massague J. Membrane-anchored and soluble forms of betaglycan, a polymorphic proteoglycan that binds transforming growth factor-β. *J Cell Biol*. 1989;109(6 Pt 1):3137-3145. doi:10.1083/jcb.109.6.3137
- Bandyopadhyay A, Wang L, Lopez-Casillas F, Mendoza V, Yeh IT, Sun L. Systemic administration of a soluble betaglycan suppresses tumor growth, angiogenesis, and matrix metalloproteinase-9 expression in a human xenograft model of prostate cancer. *Prostate*. 2005;63(1):81-90. doi:10.1002/pros.20166
- Hernandez-Pando R, Orozco-Esteves H, Maldonado HA, et al. A combination of a transforming growth factor-β antagonist and an inhibitor of cyclooxygenase is an effective treatment for murine pulmonary tuberculosis. *Clin Exp Immunol*. 2006;144(2):264-272. doi:10.1111/j.1365-2249.2006.03049.x
- Juarez P, Vilchis-Landeros MM, Ponce-Coria J, et al. Soluble betaglycan reduces renal damage progression in db/db mice. *Am J Physiol Renal Physiol*. 2007;292(1):F321-F329. doi:10.1152/ajprenal.00264.2006
- Vilchis-Landeros MM, Montiel JL, Mendoza V, Mendoza-Hernandez G, Lopez-Casillas F. Recombinant soluble betaglycan is a potent and isoform-selective transforming growth factor-β neutralizing agent. *Biochem J*. 2001;355(Pt 1):215-222. doi:10.1042/0264-6021:3550215
- Andres JL, DeFalcis D, Noda M, Massague J. Binding of two growth factor families to separate domains of the proteoglycan betaglycan. *J Biol Chem*. 1992;267(9):5927-5930.
- Jenkins LM, Horst B, Lancaster CL, Myhre K. Dually modified transmembrane proteoglycans in development and disease. *Cytokine Growth Factor Rev*. 2018;39:124-136. doi:10.1016/j.cytogfr.2017.12.003
- Jenkins LM, Singh P, Varadaraj A, et al. Altering the proteoglycan state of transforming growth factor β type III receptor



- (TbetaRIII)/betaglycan modulates canonical Wnt/beta-catenin signaling. *J Biol Chem.* 2016;291(49):25716-25728. doi:10.1074/jbc.M116.748624
14. Stenvers KL, Tursky ML, Harder KW, et al. Heart and liver defects and reduced transforming growth factor b2 sensitivity in transforming growth factor b type III receptor-deficient embryos. *Mol Cell Biol.* 2003;23(12):4371-4385.
  15. Clark CR, Robinson JY, Sanchez NS, et al. Common pathways regulate type III TGFbeta receptor-dependent cell invasion in epicardial and endocardial cells. *Cell Signal.* 2016;28(6):688-698. doi:10.1016/j.cellsig.2016.03.004
  16. Compton LA, Potash DR, Brown CB, Barnett JV. Coronary vessel development is dependent on the type III transforming growth factor  $\beta$  receptor. *Circ Res.* 2007;101:784-791.
  17. Sanford LP, Ormsby I, Gittenberger-de Groot AC, et al. TGFb2 knockout mice have multiple developmental defects that are non-overlapping with other TGFb knockout phenotypes. *Development.* 1997;124:2659-2670.
  18. Kamaid A, Molina-Villa T, Mendoza V, et al. Betaglycan knock-down causes embryonic angiogenesis defects in zebrafish. *Genesis.* 2015;53(9):583-603. doi:10.1002/dvg.22876
  19. Molina-Villa T, Ramírez-Vidal L, Mendoza V, Escalante-Alcalde D, López-Casillas F. Chordacentrum mineralization is delayed in zebrafish betaglycan-null mutants. *Dev Dyn.* 2022; 251(1):213-225. doi:10.1002/dvdy.393
  20. Driever W, Rangini Z. Characterization of a cell line derived from zebrafish (*Brachydanio rerio*) embryos. *In Vitro Cell Dev Biol Anim.* 1993;29A(9):749-754. doi:10.1007/BF02631432
  21. Cartharius K, Frech K, Grote K, et al. MatInspector and beyond: promoter analysis based on transcription factor binding sites. *Bioinformatics.* 2005;21(13):2933-2942. doi:10.1093/bioinformatics/bti473
  22. Ji C, Chen Y, McCarthy TL, Centrella M. Cloning the promoter for transforming growth factor-b type III receptor. Basal and conditional expression in fetal rat osteoblasts. *J Biol Chem.* 1999;274(43):30487-30494.
  23. López-Casillas F, Riquelme C, Pérez-Kato Y, et al. Betaglycan expression is transcriptionally up-regulated during skeletal muscle differentiation. *J Biol Chem.* 2003;278(1):382-390.
  24. Kwan KM, Fujimoto E, Grabher C, et al. The Tol2kit: a multi-sire gateway-based construction kit for Tol2 transposon transgenesis constructs. *Dev Dyn.* 2007;236:3088-3099. doi:10.1002/dvdy.21343
  25. Devoto SH, Melancon E, Eisen JS, Westerfield M. Identification of separate slow and fast muscle precursor cells in vivo, prior to somite formation. *Development.* 1996;122(11):3371-3380. doi:10.1242/dev.122.11.3371
  26. Barresi MJ, Stickney HL, Devoto SH. The zebrafish slow-muscle-omitted gene product is required for Hedgehog signal transduction and the development of slow muscle identity. *Development.* 2000;127(10):2189-2199.
  27. Bates D, Mächler M, Bolker B, Walker S. Fitting linear mixed-effects models using lme4. *J Stat Softw.* 2015;67(1):1-48. doi:10.18637/jss.v067.i01
  28. Bolt CC, Duboule D. The regulatory landscapes of developmental genes. *Development.* 2020;147(3):1-7. doi:10.1242/dev.171736
  29. Wu P, Yong P, Zhang Z, et al. Loss of myomixer results in defective myoblast fusion, impaired muscle growth, and severe myopathy in zebrafish. *Marine Biotechnol.* 2022;24(5):1023-1038. doi:10.1007/s10126-022-10159-3
  30. Buckingham M, Vincent SD. Distinct and dynamic myogenic populations in the vertebrate embryo. *Curr Opin Genet Dev.* 2009;19(5):444-453. doi:10.1016/j.gde.2009.08.001
  31. Hirsinger E, Stellabotte F, Devoto SH, Westerfield M. Hedgehog signaling is required for commitment but not initial induction of slow muscle precursors. *Dev Biol.* 2004;275(1):143-157. doi:10.1016/j.ydbio.2004.07.030
  32. Liew HP, Choksi SP, Wong KN, Roy S. Specification of vertebrate slow-twitch muscle fiber fate by the transcriptional regulator Blimp1. *Dev Biol.* 2008;324(2):226-235. doi:10.1016/j.ydbio.2008.09.020
  33. Ono Y, Yu W, Jackson HE, Parkin CA, Ingham PW. Adaxial cell migration in the zebrafish embryo is an active cell autonomous property that requires the Prdm1a transcription factor. *Differentiation.* 2015;89(3-4):77-86. doi:10.1016/j.diff.2015.03.002
  34. Baxendale S, Davison C, Muxworthy C, Wolff C, Ingham PW, Roy S. The B-cell maturation factor Blimp-1 specifies vertebrate slow-twitch muscle fiber identity in response to Hedgehog signaling. *Nat Genet.* 2004;36(1):88-93. doi:10.1038/ng1280
  35. von Hofsten J, Elworthy S, Gilchrist MJ, Smith JC, Wardle FC, Ingham PW. Prdm1- and Sox6-mediated transcriptional repression specifies muscle fibre type in the zebrafish embryo. *EMBO Rep.* 2008;9(7):683-689. doi:10.1038/embor.2008.73
  36. Jackson HE, Ingham PW. Control of muscle fibre-type diversity during embryonic development: the zebrafish paradigm. *Mech Dev.* 2013;130(9-10):447-457. doi:10.1016/j.mod.2013.06.001
  37. Elworthy S, Hargrave M, Knight R, Mebus K, Ingham PW. Expression of multiple slow myosin heavy chain genes reveals a diversity of zebrafish slow twitch muscle fibres with differing requirements for Hedgehog and Prdm1 activity. *Development.* 2008;135(12):2115-2126. doi:10.1242/dev.015719
  38. Roy S, Wolff C, Ingham PW. The u-boot mutation identifies a Hedgehog-regulated myogenic switch for fiber-type diversification in the zebrafish embryo. *Genes Dev.* 2001;15(12):1563-1576. doi:10.1101/gad.195801
  39. White RJ, Collins JE, Sealy IM, et al. A high-resolution mRNA expression time course of embryonic development in zebrafish. *Elife.* 2017;6:e30860. doi:10.7554/elife.30860 <http://europepmc.org/abstract/MED/29144233>
  40. Bhat P, Cabrera-Quio LE, Herzog VA, Fasching N, Pauli A, Ameres SL. SLAMseq resolves the kinetics of maternal and zygotic gene expression during early zebrafish embryogenesis. *Cell Rep.* 2023;42(2):112070. doi:10.1016/j.celrep.2023.112070
  41. Bentzinger CF, Wang YX, Rudnicki MA. Building muscle: molecular regulation of myogenesis. *Cold Spring Harb Perspect Biol.* 2012;4(2):1-16. doi:10.1101/cshperspect.a008342
  42. Nord H, Burguiere AC, Muck J, Nord C, Ahlgren U, von Hofsten J. Differential regulation of myosin heavy chains defines new muscle domains in zebrafish. *Mol Biol Cell.* 2014; 25(8):1384-1395. doi:10.1091/mbc.E13-08-0486
  43. Stapornwongkul KS, Briscoe J. In preprints: morphogens in motion. *Development.* 2022;149(14):1-2. doi:10.1242/dev.201066
  44. Stapornwongkul KS, Vincent JP. Generation of extracellular morphogen gradients: the case for diffusion. *Nat Rev Genet.* 2021;22(6):393-411. doi:10.1038/s41576-021-00342-y

45. Harish RK, Gupta M, Zöller D, et al. Real-time monitoring of endogenous Fgf8a gradient attests to its role as a morphogen during zebrafish gastrulation. *bioRxiv*. 2022:2022.04.26.488902. doi:[10.1101/2022.04.26.488902](https://doi.org/10.1101/2022.04.26.488902)
46. Brûlé E, Wang Y, Li Y, et al. TGFBR3L is an inhibin B co-receptor that regulates female fertility. *Sci Adv*. 2021;7(51):eabl4391. doi:[10.1126/sciadv.abl4391](https://doi.org/10.1126/sciadv.abl4391)
47. Westerfield M. *The Zebrafish Book. A Guide for the Laboratory Use of Zebrafish (Danio rerio)*. 4th ed. Oregon, USA: University of Oregon Press; 2000.
48. Kimmel CB, Ballard WW, Kimmel SR, Ullmann B, Schilling TF. Stages of embryonic development of the zebrafish. *Dev Dyn*. 1995;203:253-310.
49. Martin CS, Wight PA, Dobretsova A, Bronstein I. Dual luminescence-based reporter gene assay for luciferase and beta-galactosidase. *Biotechniques*. 1996;21(3):520-524. doi:[10.2144/96213pf01](https://doi.org/10.2144/96213pf01)
50. Smale ST. Luciferase assay. *Cold Spring Harb Protoc*. 2010;2010(5):pdb prot5421. doi:[10.1101/pdb.prot5421](https://doi.org/10.1101/pdb.prot5421)
51. Langmead B, Salzberg SL. Fast gapped-read alignment with Bowtie 2. *Nat Methods*. 2012;9(4):357-359. doi:[10.1038/nmeth.1923](https://doi.org/10.1038/nmeth.1923)
52. Ramírez F, Ryan DP, Grüning B, et al. deepTools2: a next generation web server for deep-sequencing data analysis. *Nucleic Acids Res*. 2016;44(W1):W160-W165. doi:[10.1093/nar/gkw257](https://doi.org/10.1093/nar/gkw257)
53. Heinz S, Benner C, Spann N, et al. Simple combinations of lineage-determining transcription factors prime cis-regulatory elements required for macrophage and B cell identities. *Mol Cell*. 2010;38(4):576-589. doi:[10.1016/j.molcel.2010.05.004](https://doi.org/10.1016/j.molcel.2010.05.004)

**How to cite this article:** Ramírez-Vidal L, Molina-Villa T, Mendoza V, et al. Betaglycan promoter activity is differentially regulated during myogenesis in zebrafish embryo somites. *Developmental Dynamics*. 2023;252(9):1162-1179. doi:[10.1002/dvdy.602](https://doi.org/10.1002/dvdy.602)